

# Field experimental study of traffic-induced turbulence on highways

Alonso-Estébanez, A, Pascual-Muñoz, P, Yagüe, C, Laina, R & Castro-Fresno, D

Author post-print (accepted) deposited by Coventry University's Repository

**Original citation & hyperlink:**

Alonso-Estébanez, A, Pascual-Muñoz, P, Yagüe, C, Laina, R & Castro-Fresno, D 2012, 'Field experimental study of traffic-induced turbulence on highways' Atmospheric Environment, vol. 61, pp. 189-196.

<https://dx.doi.org/10.1016/j.atmosenv.2012.07.032>

DOI 10.1016/j.atmosenv.2012.07.032

ISSN 1352-2310

Publisher: Elsevier

**NOTICE: this is the author's version of a work that was accepted for publication in Atmospheric Environment Changes resulting from the publishing process, such as peer review, editing, corrections, structural formatting, and other quality control mechanisms may not be reflected in this document. Changes may have been made to this work since it was submitted for publication. A definitive version was subsequently published in Atmospheric Environment [61 (2012)] DOI: 10.1016/j.atmosenv.2012.07.032**

© 2017, Elsevier. Licensed under the Creative Commons Attribution-NonCommercial-NoDerivatives 4.0 International

<http://creativecommons.org/licenses/by-nc-nd/4.0/>

Copyright © and Moral Rights are retained by the author(s) and/ or other copyright owners. A copy can be downloaded for personal non-commercial research or study, without prior permission or charge. This item cannot be reproduced or quoted extensively from without first obtaining permission in writing from the copyright holder(s). The content must not be changed in any way or sold commercially in any format or medium without the formal permission of the copyright holders.

This document is the author's post-print version, incorporating any revisions agreed during the peer-review process. Some differences between the published version and this version may remain and you are advised to consult the published version if you wish to cite from it.

# Field experimental study of traffic-induced turbulence on highways

A. Alonso-Estébanez<sup>a</sup>, P. Pascual-Muñoz<sup>b</sup>, C. Yagüe<sup>c</sup>, R. Laina<sup>d</sup>, D. Castro-Fresno<sup>e,\*</sup>

<sup>a</sup>Dept. of Transport, Project and Process Technology, ETSICCP, Univ. of Cantabria, Ave. Castros s/n, 39005 Santander, Spain. E-mail: alonsoea@unican.es.

<sup>b</sup>Dept. of Transport, Project and Process Technology, ETSICCP, Univ. of Cantabria, Ave. Castros s/n, 39005 Santander, Spain. E-mail: pascualmp@unican.es

<sup>c</sup>Dpto. Geofísica y Meteorología, Fac. C. Físicas, Universidad Complutense de Madrid, Ciudad Universitaria, Plaza de Ciencias, 1, 28040 Madrid, Spain. E-mail: carlos@fis.ucm.es.

<sup>d</sup>Dept. of R&D, OHL Concessions, Paseo de la Castellana 259 D, 28046 Madrid, Spain. E-mail: rlaina@ohlconcesiones.com.

<sup>e</sup>Dept. of Transport, Project and Process Technology, ETSICCP, Univ. of Cantabria, Ave. Castros s/n, 39005 Santander, Spain. E-mail: castrod@unican.es.

\*Corresponding author. Tel.: +34 942 203943; fax: +34 942 201703.

## Abstract

This paper is focused on traffic-induced turbulence (TIT) analysis from a field campaign performed in 2011, using ultrasonic anemometers deployed in the M-12 Highways, Madrid (Spain). The study attempts to improve knowledge about the influence of traffic-related parameters on turbulence. Linear relationships between vehicle speed and turbulent kinetic energy (*TKE*) values are found with coefficients of determination ( $R^2$ ) of 0.75 and 0.55 for the lorry and van respectively. The vehicle-induced fluctuations in the wind components ( $u'$ ,  $v'$  and  $w'$ ) showed the highest values for the longitudinal component ( $v'$ ) because of the wake-passing effect. In the analysis of wake produced by moving vehicles it is indicated how the turbulence dissipates in relation to a distance  $d$  and height  $h$ . The *TKE* values were found to be higher at the measuring points closer to the surface during the wake analysis.

*Keywords:* Vehicle-induced turbulence; parameterization; highway turbulence; turbulence intensity

## 1. Introduction

Pollutant emissions from vehicles are a significant issue in relation to the environment and human health. Occasionally these contaminants are dispersed by the wind from roads to population centers. Therefore, better knowledge of the turbulence processes that are involved in the environment of roads is valuable in the definition of new pollutant diffusion models. One of the sources in the generation of turbulence is vehicle

39 traffic (Rao et al., 1979). Some researchers have shown that the pollutant dispersion  
40 models that consider in detail the traffic-induced turbulence (TIT) effects provide a  
41 better fit with field measurements, than other models as CALINE4 and CFD models  
42 without this consideration (Wang and Zhang, 2009 and Sahlodin et al., 2007). In  
43 conditions of low wind velocity and wind direction perpendicular to the road, the traffic  
44 contribution to diffusion of pollutants still remains above 50% at 30m away downwind  
45 of the road (Sedefian et al., 1981).

46

47 As a result, some researchers have studied TIT from different perspectives. A  
48 theoretical analysis of the vehicle wake was carried out by Eskridge and Hunt (1979).  
49 This research proposes some equations for velocity of the vehicle wake from  
50 fundamental motion equations. Hider et al. (1997) extended the wake formulation in  
51 conditions of lateral and vertical wind using the main equations of Eskridge and Hunt  
52 (1979). Field experiments were also carried out in which the vehicle wake is analyzed  
53 according to different methodologies (Chock, 1980; Rao et al., 2002). Rao et al. (2002)  
54 installed anemometers on the back of moving vehicles to measure the turbulence just  
55 behind of the vehicle while Chock (1980) located anemometers on both sides of the  
56 road to measure turbulence parameters in the lee/windward side of the highway. They  
57 found that wind direction perpendicular to the road increases TIT effects.

58

59 TIT was also analyzed in wind tunnel installations (Eskridge and Thomson, 1982)  
60 although turbulence generation systems required improvement since occasional  
61 differences between measurements in field campaigns and in wind tunnels have been  
62 found (Cooper and Campbell, 1981). Cooper and Campbell (1981) used wind-tunnel  
63 and full-scale measurements of the aerodynamic drag on trucks to show the influence of  
64 wind turbulence. In addition a quasi-steady theory is developed to consider the effects  
65 of turbulence. Watkins et al. (1995) explained how to improve the similarity between  
66 turbulence levels in wind tunnels and in the field through structural elements.

67

68 Urban street canyons in cities are locations with high concentrations of contaminants  
69 because the air flows are smooth in these sheltered zones (Jicha et al., 2000; Vachon et  
70 al., 2000; Kastner-Klein et al., 2001; Longley et al., 2004). Kastner-Klein et al. (2001)  
71 showed how traffic affects the turbulent airflow in canyons by means of wind tunnel  
72 tests. Recently, some researchers (Jicha et al., 2000; Katolicky and Jicha 2005; Dong

73 and Chan 2006; Xia et al., 2006; Sahlodin et al., 2007) have studied the turbulent  
74 process relative to the traffic using CFD (Computational Fluid Dynamics) codes  
75 because of the good fit with field measurements. Katolicky and Jicha (2005) showed  
76 that if TIT is included in atmospheric turbulence models (e.g. using a  $k-\varepsilon$  model), the air  
77 flow in canyons increases by 10%, so pollutant concentrations decrease.

78

79 In addition to TIT, the roads themselves influence and modify the flow and turbulence,  
80 the additionally generated turbulence being of significance for pollutant dispersion  
81 (Kalthoff et al., 2005).

82

83 Thermally induced turbulence can also be produced due to the presence of highways, as  
84 sensitive and latent heat fluxes are different compared to those coming from natural  
85 environments (Oke, 1987; Kalthoff et al., 1991). However, the influence on the  
86 production of turbulent kinetic energy ( $TKE$ ) seems to be smaller compared to dynamic  
87 effects (Weiß, 2002; Kalthoff et al., 2005).

88

89 In this paper, TIT is analyzed in a field experiment. The experiment shows the  
90 relationship of turbulent parameters with vehicle type and speed and how TIT varies  
91 with the perpendicular distance to vehicles on their leeward side. The first part of the  
92 paper describes the experimental setup and the turbulence measurement, and the second  
93 part presents and discusses the results of the experiment. The main goal is to improve  
94 knowledge about TIT in space near vehicles and how different parameters affect it.

95

## 96 **2. Methodology and experimental setup**

97 Wind velocity variances ( $\sigma$ ) registered from fixed points on the highway are produced  
98 by ambient and vehicle turbulence (Kalthoff et al., 2005). The ambient turbulence,  
99 produced within the so-called Atmospheric Boundary Layer (ABL), is caused  
100 mechanically by wind shear and buoyancy induced by thermals (Stull, 1988). It is  
101 common practice in turbulent flows to express variables (temperature, velocity, etc.) as  
102 sums of mean and fluctuating parts (Arya, 2001):

$$u = u' + \bar{u} \quad (1)$$

103 Two kinds of velocity fluctuations are recorded by a fixed anemometer on road when  
104 moving vehicles pass by it: the wake when the wind hits the vehicle as an obstacle and

105 the wake-passing effect which is specifically generated by moving vehicles, even in the  
106 absence of wind (Eskridge and Rao, 1983). Parameters such as the turbulent momentum  
107 fluxes (e.g.  $\overline{u'v'}$ ) involving covariance between velocity component fluctuations, and the  
108 *TKE* defined as:

$$TKE = 0.5(\sigma_u^2 + \sigma_v^2 + \sigma_w^2) \quad (2)$$

109 may be interesting to analyze TIT. Variances of wind components ( $\sigma_u^2$ ,  $\sigma_v^2$  and  $\sigma_w^2$ )  
110 are directly related to the three wind component perturbations:

$$\begin{aligned} \sigma_u^2 &= \overline{u'^2} \\ \sigma_v^2 &= \overline{v'^2} \\ \sigma_w^2 &= \overline{w'^2} \end{aligned} \quad (3)$$

111 Where  $u$ ,  $v$  and  $w$  are the perpendicular, longitudinal and vertical directions relative to  
112 the highway. The TIT measuring campaign presented in this work was supported by the  
113 first Spanish project on future highway design, OASIS ([www.cenitoasis.com](http://www.cenitoasis.com)).

114

#### 115 *2.1. Experimental setup: M-12*

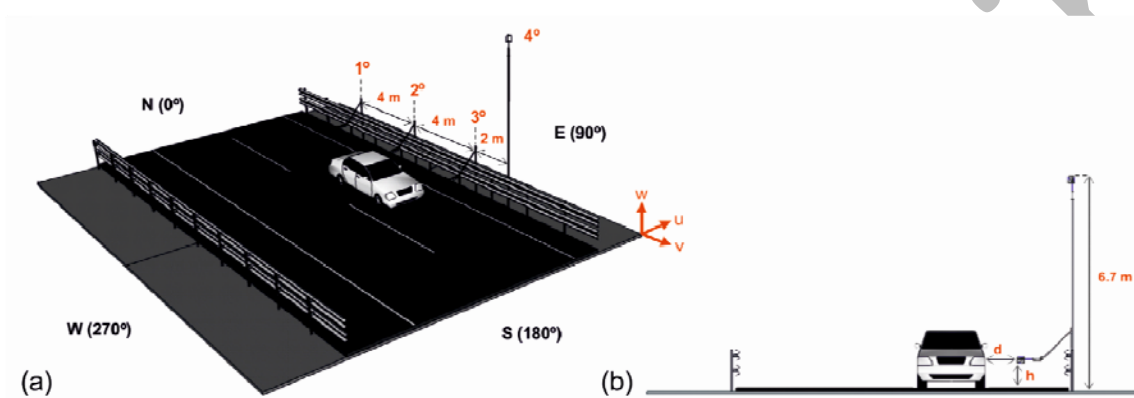
116 Highway M-12 near Madrid airport was the location to carry out the experiment from 2  
117 to 4th August 2011. This highway has two lanes running from North (0°) to South  
118 (180°) and is limited by guardrails (Fig. 1). A toll booth with twelve lanes is located on  
119 the east side of the experimental setup and flat land is found to the west. The  
120 surroundings are quite flat with small embankments. The location was chosen because it  
121 has low traffic density and a long straight section, which facilitates the different  
122 experimental procedures. The Spanish Meteorological Agency (AEMET) has a  
123 measuring station situated approximately at 2.4km from the experimental site. In this  
124 station (Barajas Airport), the climatological (1971-2000) wind direction in August is  
125 from NE with a  $3\text{m s}^{-1}$  mean wind velocity.

126

127 The M-12 experiment was divided into three different tests. In all tests, four Gill  
128 ultrasonic anemometers (Wind Master model) with a maximum sample frequency of  
129 20Hz and a resolution of  $0.01\text{m s}^{-1}$  were used. Three of them were installed on the  
130 guardrails maintaining a distance among them of 4m and their heights  $h$  and distances  $d$   
131 (Fig. 1) were set depending on the test being done. The fourth anemometer was located  
132 at a height of 6.7m in order to measure ambient wind (Fig. 1), this height is beyond the  
133 influence of traffic according to Eskridge and Thompson (1982).

134

135 Test-1 studies how the wake-passing effect behaves at different heights. Anemometers  
136 1, 2 and 3 were installed at heights  $h$  (Fig. 1) of  $0.25H_{\text{vehicle}}$ ,  $0.75H_{\text{vehicle}}$  and  $1.25H_{\text{vehicle}}$   
137 ( $H_{\text{vehicle}}$  is the vehicle height), respectively (Table 1). The vehicle heights for car and  
138 lorry are respectively 1.4m and 3.2m. The minimum horizontal distance between the  
139 vehicle trajectory and anemometer  $d$  (Fig. 1) was approximately 1m. For this test, a car  
140 and a lorry (Fig. 2a and Fig. 2c) were used; both vehicles performed 3 runs at 90km/h.



141

142

143

Fig. 1. Sketch of the experiment with the position of four ultrasonic anemometers on the highway M-12. (a) Perspective view and (b) frontal view.



144

145

146

Fig. 2. Vehicle classes used in the experiment: (a) Car, (b) Van and (c) Lorry.

147

148

149

150

151

152

153

Test-2 was designed to show how vehicle speed and vehicle type relate with turbulence parameters. Anemometers 1, 2 and 3 were installed at a level of 0.7m and the distance was the same as for Test-1 for all anemometers (Table 1). A van with a  $H_{\text{vehicle}}$  of 2.6m (Fig. 2b) a car and a lorry, were included in the experiment, to establish the influence of an intermediate size. All vehicles performed 3 runs each, at speeds of 90km/h, 80km/h, 70km/h and 60km/h.

154

155

156

157

Test-3 aimed to analyze how TIT ranges with the distance,  $d$  (Fig. 1). Anemometers 1, 2 and 3 were placed at a height of 0.7m while the separation distances were 1m, 2.2m and 3.4m respectively (Table 1). The lorry was chosen to perform 3 runs at 90km/h, because it had caused the strongest turbulence in the previous tests.

158  
159

**Table 1**  
**Position of anemometers on highway M-12 during each test.**

Test	$d_1^a$ (m)	$d_2^a$ (m)	$d_3^a$ (m)	$h_1^b$ (m)	$h_2^b$ (m)	$h_3^b$ (m)
1	1	1	1	$0.25H_{\text{vehicle}}$	$0.75H_{\text{vehicle}}$	$1.25H_{\text{vehicle}}$
2	1	1	1	0.7	0.7	0.7
3	3.4	2.2	1	0.7	0.7	0.7

<sup>a</sup>Minimum horizontal distance between the anemometers and the trajectory of vehicles (Fig. 1).

<sup>b</sup>Height over ground (Fig. 1).

160 The anemometers were sampled at 20Hz during a period of 120sec. The maximum  
161 fluctuating components ( $u'_{\max}$ ,  $v'_{\max}$ ,  $w'_{\max}$ ), *TKE* and turbulent momentum fluxes were  
162 obtained in the time range from when the vehicle passed anemometer 1 (Fig. 1) until the  
163 vehicle covered 230m. Some parameters were normalized with the average of the  
164 perpendicular component,  $U$  from anemometer 4 (Fig. 1). A correlation analysis  
165 between study parameters was carried out for all tests with SPSS (statistical software).  
166 The Pearson correlation was obtained to reflect the degree to which the variables are  
167 related. This parameter ranges from +1 to -1. A correlation value equal to +1 means that  
168 there is a perfect positive linear relationship between variables. Sometimes vehicles not  
169 involved in the test coincided with the test vehicles and these runs were rejected. Other  
170 runs were not analyzed because of signal errors.

171

### 172 3. Results and discussion

173 Unlike other studies, such as Kalthoff et al. (2005) and Chock (1980), the present  
174 research is oriented to analyzing TIT near traffic.

175 As was indicated (*Experimental setup: M-12*), three tests were run within the  
176 experiment. Now the results of these different tests will be analyzed.

177

#### 178 3.1. Test-1: Height dependence

179 This test attempts to illustrate how the wake-passing effect changes at different heights.

180 Therefore, the relationship between turbulence parameters and height will be studied.

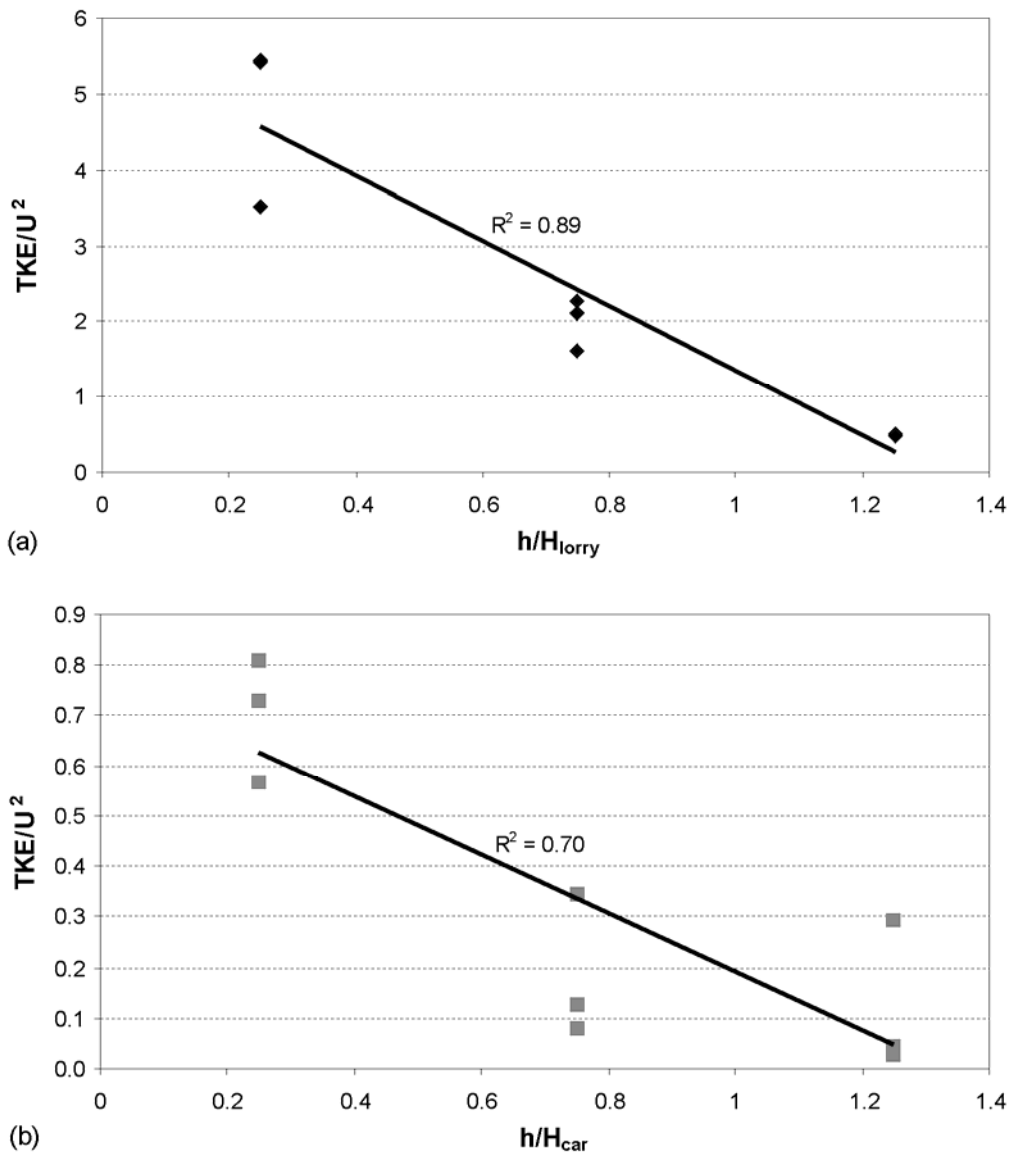
181 *TKE* values significantly correlated well with the height parameter,  $h$  (Fig. 1) in the car  
182 and lorry cases, where the Pearson correlation coefficients were -0.84 and -0.94  
183 respectively (Fig. 3). The turbulence is stronger near the road surface, which may be  
184 due to ground roughness and the guardrail's effect. The larger size of the lorry induces a  
185 higher momentum interchange between it and the surrounding air and the *TKE* values  
186 obtained during lorry runs were about 10 times higher than in car runs. The slope for the

187 lorry fit is larger than that corresponding to the car, indicating the stronger vertical  
 188 gradient in the  $TKE$  for the lorry case. Two simple linear models describe the  
 189 relationship between the  $TKE$  parameter and height,  $h$  for both kinds of vehicles. The  
 190 coefficient of determination  $R^2$  for the lorry model is 0.89 and in the case of the car is  
 191 0.70 (Fig. 3). The linear fits obtained for the lorry and the car are

$$TKE/U^2 = 5.66 - 4.30h/H_{lorry} \quad (4)$$

192 and

$$TKE/U^2 = 0.77 - 0.58h/H_{car} \quad (5)$$

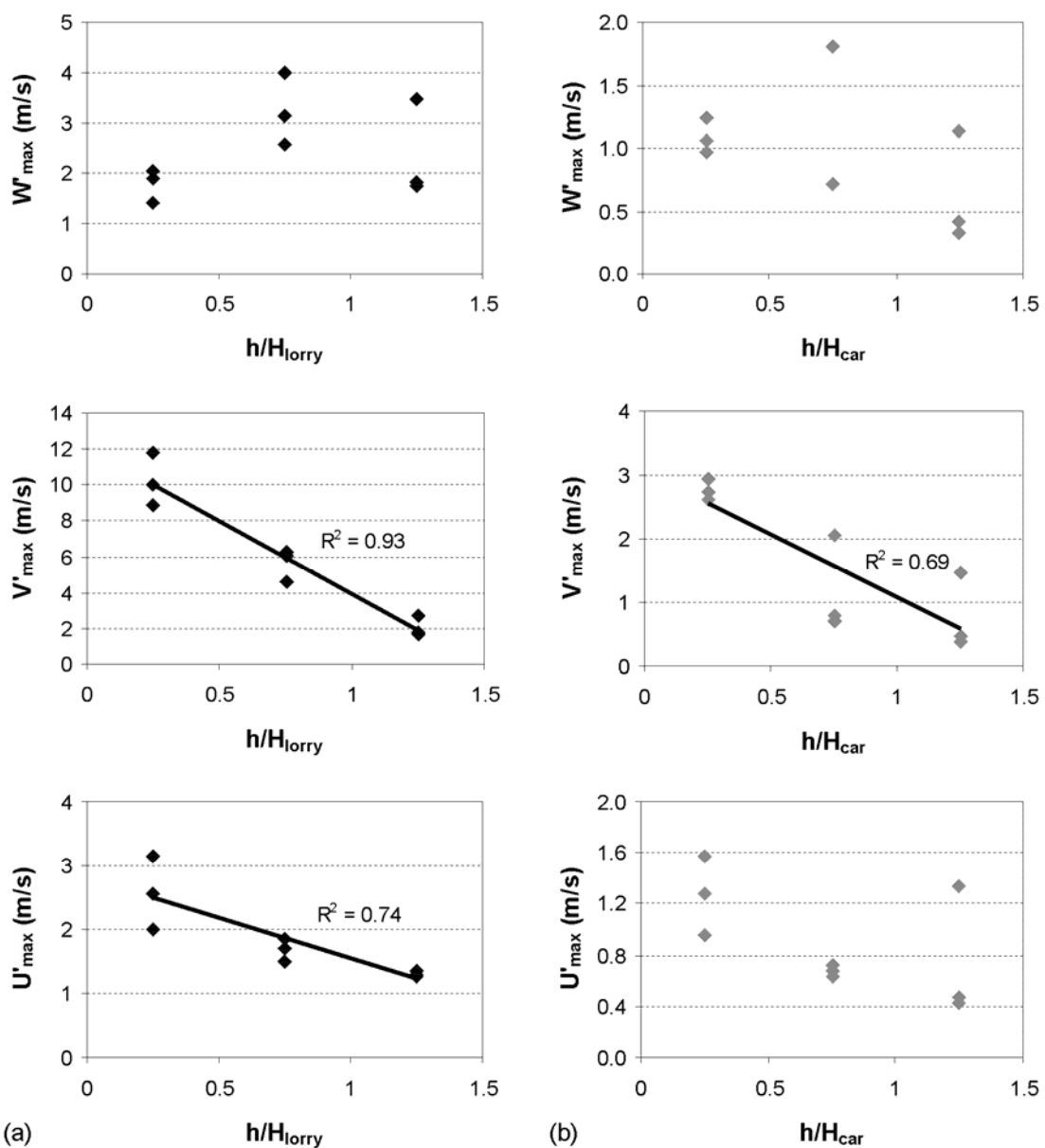


193 Fig. 3. Normalized  $TKE$  values depending on the height ratios (Table 1) of both the lorry (a) and the  
 194 car (b).  
 195

196 Fig. 4 shows how the longitudinal component ( $v$ ) undergoes the maximum fluctuation  
 197 compared to the other components ( $u$ ,  $w$ ). This is caused by the wake-passing effect.



198 Thus turbulence originated from vehicles exhibits a strong anisotropy. In the lorry case  
 199 both the longitudinal and perpendicular components significantly correlate with the  
 200 height ratio, while in the car case only with the longitudinal component (Fig. 4). In  
 201 addition the vertical fluctuating component is independent of the height for both  
 202 vehicles. Moreover, Eskridge and Rao (1983) also found that the fluctuating component  
 203 with highest values was longitudinal. Therefore, the highest proportion of *TKE* is  
 204 caused by the turbulent flow induced in the vehicle path. The coefficient of  
 205 determination,  $R^2$  is not shown in some graphics (Fig. 4) because the correlation  
 206 between those variables is not significant.



207 (a) (b)  
 208 Fig. 4. Relationship between maximum fluctuation of components and height ratio for both the  
 209 lorry (a) and the car cases (b).  
 210

211 3.2. *Test-2: Speed and volume dependence*

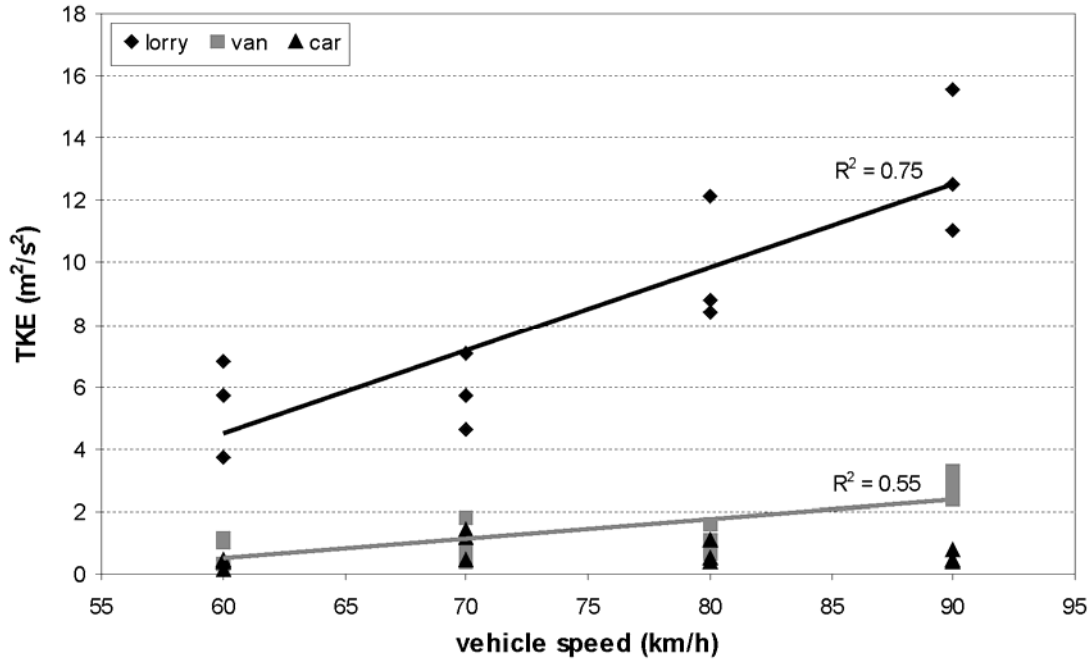
212 The total drag on a vehicle essentially consists of the friction and pressure drags  
213 (Geropp and Odenthal, 2000) and it increases with vehicle speed. Therefore, the  
214 momentum transfer from vehicle to air through friction and pressure drags must also  
215 increase with speed and vehicle size. This test includes an intermediate vehicle size in  
216 relation to ***Test-1: Height dependence***, a van. Values of wake-passing effect are  
217 obtained from 3 anemometers located at a height of 0.7m. Both the lorry and the van  
218 show a significant Pearson correlation between *TKE* and vehicle speed, whose values  
219 are 0.86 (lorry) and 0.74 (van). The linear models obtained from the fits to the data (Fig.  
220 5) for the lorry and van, are

$$TKE = -11.60 + 0.27V \quad (6)$$

221 and

$$TKE = -3.19 + 0.06V \quad (7)$$

222 where  $V$  is vehicle speed and the coefficients of determination  $R^2$  are 0.75 and 0.55  
223 respectively. The *TKE* values obtained for the lorry are much larger than those reached  
224 with the van and car, the increase produced as the vehicle increases its speed also being  
225 greater, so the turbulence produced by the lorry becomes much more influential than the  
226 other two vehicles as the speed increases. Even, for the car case *TKE* values do not  
227 exhibit distinct functional relationship with vehicle speed. The differences of *TKE*  
228 values between lorry and the other vehicles will diminish if the lorry has a better  
229 aerodynamics with lower drag coefficient. Since the streamlines could keep better close  
230 to lorry's surface.



231

232 **Fig. 5. TKE depending on the vehicle speed for different kinds of vehicles.**

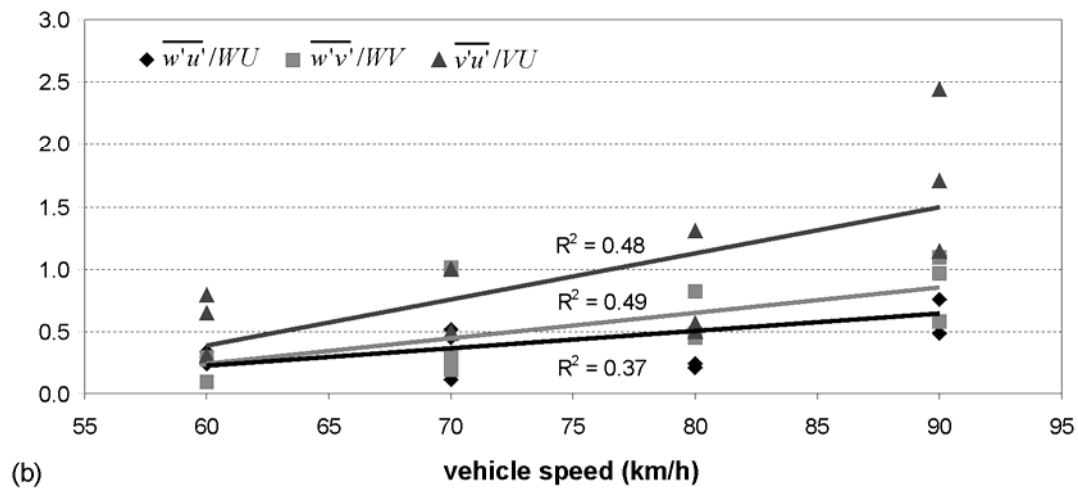
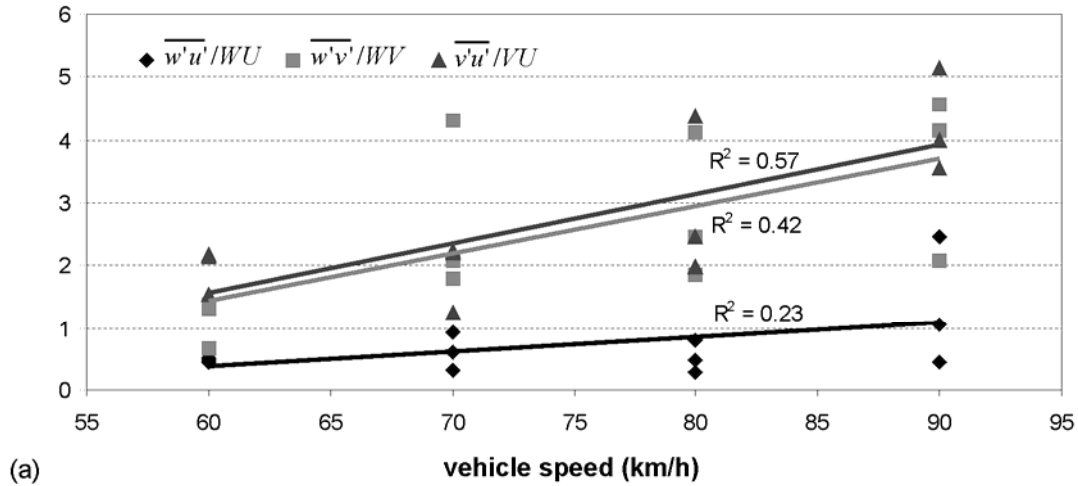
233 Turbulent momentum fluxes involve covariance between velocity fluctuations in  
 234 different directions (Arya, 2001). The matrix is shaped by the nine momentum fluxes in  
 235 relation to combinations among components. In order to analyze the covariance between  
 236 the three components of the flow, only off-diagonal components:  $\overline{w'u'}$ ,  $\overline{w'v'}$  and  $\overline{v'u'}$ ,  
 237 have been calculated. These components contribute to the transport of mean momentum  
 238 while diagonal components are related to *TKE*, as was described in eq. (2) (Tennekes  
 239 and Lumley, 1972).

240

241 The longitudinal fluxes of vertical and perpendicular momentum ( $\overline{w'v'}$ ,  $\overline{u'v'}$ ) have the  
 242 highest values and better correlation both for the lorry and van (Fig. 6). Again, this is  
 243 because of the higher fluctuations in the longitudinal component ( $v'$ ).

244 As, in a non-perturbed ABL (Atmospheric Boundary Layer), vertical transfer of  
 245 momentum ( $v'w'$ ,  $u'w'$ ) is usually much larger than horizontal fluxes ( $u'v'$ ), especially  
 246 in homogeneous terrain (Stull, 1988; Arya, 2001; Wyngaard, 2010), the results obtained  
 247 are clearly influenced by TIT. All momentum fluxes smoothly increase with vehicle  
 248 speed, but all coefficients of determination  $R^2$  are quite low. Results from the car case  
 249 are not shown because no correlation is found ( $R^2 < 0.009$ ). The vertical fluxes of  
 250 longitudinal momentum,  $\overline{v'w'}$  exhibit the highest differences between the lorry and van.

251



252  
253 **Fig. 6. Variation of normalized turbulent momentum fluxes with vehicle speed for the lorry (a) and**  
254 **van case (b).**

256 The normalized turbulent fluxes that show highest Pearson correlations with vehicle  
257 speed are  $\overline{w'v'}/WV$  for the van and  $\overline{v'u'}/VU$  for the lorry (Table 2).

258  
259 **Table 2**  
260 **Pearson correlation between normalized turbulent momentum fluxes and vehicle speed.**

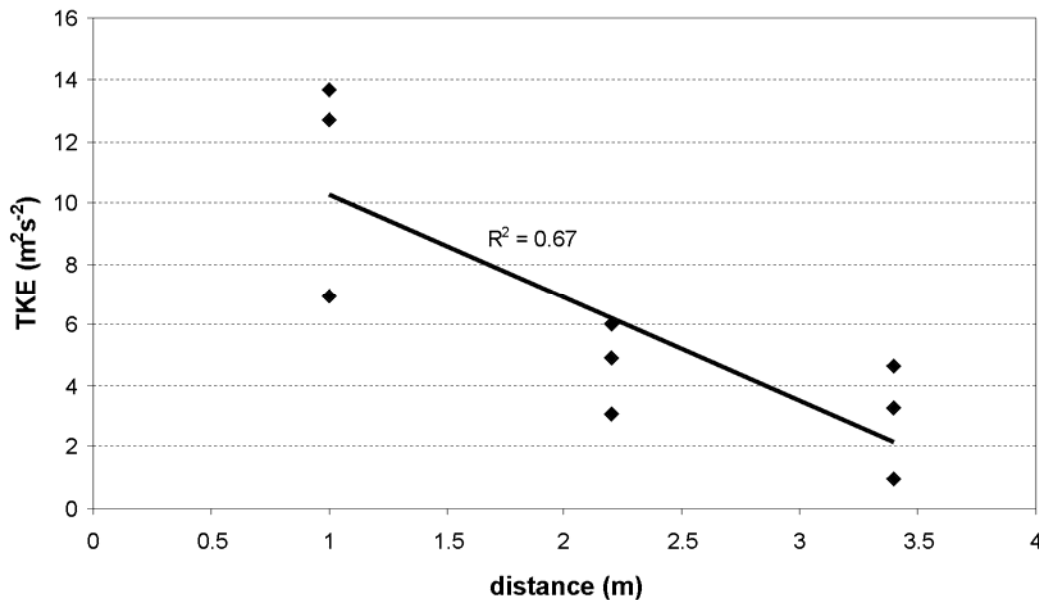
	Pearson Correlation		
	$\overline{w'u'}/WU$	$\overline{w'v'}/WV$	$\overline{v'u'}/VU$
Vehicle speed (Lorry)	0.48	0.65 <sup>a</sup>	0.76 <sup>a</sup>
Vehicle speed (Van)	0.61 <sup>a</sup>	0.70 <sup>a</sup>	0.69 <sup>a</sup>

<sup>a</sup>The correlation is significant with 95% probability.

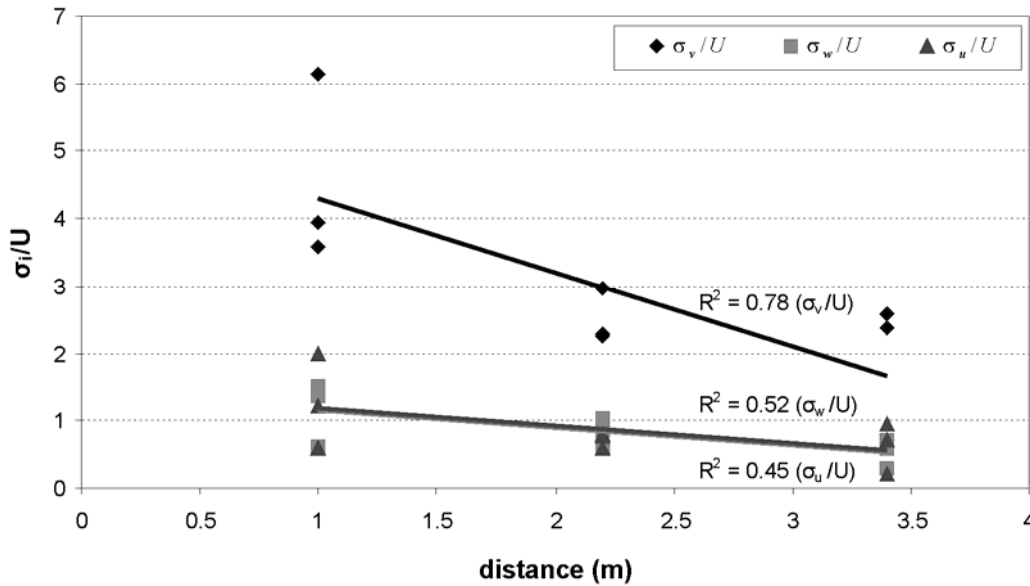
261  
262 **3.3. Test-3: Distance dependence**

263 The lorry was chosen for this test because it helps to better distinguish the vehicle  
264 turbulence from ambient turbulence; moreover, it produces much more turbulence. This

265 test attempts to demonstrate how the wake from a moving vehicle dissipates over  
 266 distance,  $d$  (Fig. 7).  $TKE$  values that were obtained at closer points to the vehicle  
 267 trajectory are higher than at farther points, as would be expected (Fig. 7). The  
 268 dissipation rate of  $TKE$  values with distance is  $-3.4\text{m}^{-1}\text{s}^{-2}$ . On the other hand, the  
 269 average of the perpendicular component,  $U$  from anemometer 4 was used to obtain the  
 270 turbulence intensities components. The longitudinal turbulence intensity ( $\sigma_v/U$ )  
 271 contributes a higher proportion to  $TKE$  values (Fig. 8). In addition this component  
 272 shows the highest coefficient of determination  $R^2$ , 0.78. Although all turbulence  
 273 intensities are correlated significantly with distance from the vehicle trajectory, the  
 274 longitudinal component decreases faster than the other components (Fig. 8). The values  
 275 of perpendicular and vertical turbulence intensity ( $\sigma_u/U$  and  $\sigma_w/U$ ) are quite similar.



276  
 277 Fig. 7. Relationship between normalised  $TKE$  values and the distance,  $d$  (Fig. 1) for the lorry case.  
 278



279 Fig. 8. Turbulence intensity components depending on the distance,  $d$  (Fig. 1) for the lorry case.  
 280  
 281

#### 282 4. Summary and Conclusions

283 Results from a field campaign to study traffic-induced turbulence (TIT) are presented in  
 284 this work. The field campaign was carried out in August 2011, with the aim of studying  
 285 the relationship between TIT and different parameters. First, the influence of parameters  
 286 related to vehicles, such as speed and size were analyzed. Second, the spatial variation  
 287 of the TIT along the perpendicular and vertical direction to vehicle trajectory is  
 288 determined. The wake-passing effect produced by the vehicles causes the longitudinal  
 289 direction to contribute the highest proportion to the  $TKE$  values for the three tests  
 290 performed. Both the turbulent momentum fluxes and the  $TKE$  values correlated well  
 291 with the vehicle speed for the lorry and the van, but not for the car, where the turbulence  
 292 produced is much lower. As would be expected, the  $TKE$  values and the coefficient of  
 293 determination  $R^2$ , found for the different fits, are higher for the lorry than for the van  
 294 and the car. The turbulent momentum fluxes, which depend on fluctuations in the  
 295 longitudinal component, are higher compared to the other directions. The Pearson  
 296 correlation coefficients between the values of  $TKE$  and the height parameter for the car  
 297 and the lorry are -0.84 and -0.94 respectively, indicating that the turbulence level  
 298 increased as the distance to the road decreases. The intensity of turbulence from the  
 299 vehicles decreases significantly with the distance perpendicular to the vehicle trajectory.  
 300 Moreover, the dissipation energy rate in the longitudinal component is higher than the  
 301 other components.  
 302

303 This analysis shows clearly that TIT can be an important source of turbulence, in  
304 addition to the natural turbulence produced in the surface layer, and it should be  
305 considered in air quality models simulating pollutant concentrations. The study also  
306 confirmed that TIT could be modelled taking into account some parameters relative to  
307 the vehicles.

308

### 309 **Acknowledgements**

310 This work was supported by the OASIS Research Project that was co financed by CDTI  
311 (Spanish Science and Innovation Ministry) and developed with the Spanish companies:  
312 Iridium, OHL Concesiones, Abertis, Sice, Indra, Dragados, OHL, Geocisa, GMV,  
313 Asfaltos Augusta, Hidrofersa, Eipsa, PyG, CPS, AEC and Torre de Comares  
314 Arquitectos s.l and 16 research centres.

315

### 316 **References**

317

318 Arya, S., 2001. Introduction to micrometeorology, second ed. Academic press, San  
319 Diego, London 420pp.

320

321 Chock, D.P., 1980. General Motor's sulfate dispersion experiment - An analysis of the  
322 wind field near a road. *Boundary-Layer Meteorology* 18, 431-451.

323

324 Cooper K.R., Campbell W.F., 1981. An examination of the effects of wind turbulence  
325 on the aerodynamic drag of vehicles. *Journal of Wind Engineering and Industrial*  
326 *Aerodynamics* 9, 167-180.

327

328 Dong G., Chan T.L., 2006. Large eddy simulation of flow structures and pollutant  
329 dispersion in the near-wake region of a light-duty diesel vehicle. *Atmospheric*  
330 *Environment* 40, 1104-1116.

331

332 Eskridge, R.E., Hunt, J.C.R., 1979. Highway modeling. Part I: Prediction of velocity  
333 and turbulence fields in the wake of vehicles. *Journal of Applied Meteorology*  
334 18, 387-400.

335

336 Eskridge R.E., Thompson R.S., 1982. Experimental and theoretical study of the wake of  
337 a block-shaped vehicle in a shear-free boundary flow. *Atmospheric Environment* 16,  
338 2821-2836.

339

340 Eskridge R.E., Rao S.T., 1983. Measurement and prediction of traffic-induced  
341 turbulence and velocity fields near roadways. *Journal of Climate & Applied*  
342 *Meteorology* 22, 1431-1443.

343

344 Geropp D., Odenthal H.J., 2000. Drag reduction of motor vehicles by active flow  
345 control using the Coanda effect. *Experiments in Fluids* 28, 74-85.

346

347 Hider Z.E., Hibberd S., Baker C.J., 1997. Modelling particulate dispersion in the wake  
348 of a vehicle. *Journal of Wind Engineering and Industrial Aerodynamics* 67-68, 733-744.  
349

350 Jicha M., Pospisil J., Katolicky J., 2000. Dispersion of pollutants in street canyon under  
351 traffic induced flow and turbulence. *Environmental Monitoring and Assessment* 65,  
352 343-351.  
353

354 Kalthoff, N., Corsmeier, U., Fiedler, F., 1991. Modification of turbulent fluxes and  
355 temperature fields in the atmospheric surface layer over two adjacent agricultural areas:  
356 a case study. *Annales Geophysicae* 9, 521-533.  
357

358 Kastner-Klein P., Fedorovich E., Rotach M.W., 2001. A wind tunnel study of organised  
359 and turbulent air motions in urban street canyons. *Journal of Wind Engineering and*  
360 *Industrial Aerodynamics* 89, 849-861.  
361

362 Kalthoff N., Baumer D., Corsmeier U., Kohler M., Vogel B., 2005. Vehicle-induced  
363 turbulence near a motorway. *Atmospheric Environment* 39, 5737-5749.  
364

365 Katolicky J., Jicha M., 2005. Eulerian-Lagrangian model for traffic dynamics and its  
366 impact on operational ventilation of road tunnels. *Journal of Wind Engineering and*  
367 *Industrial Aerodynamics* 93, 61-77.  
368

369 Longley I.D., Gallagher M.W., Dorsey J.R., Flynn M., Barlow J.F., 2004. Short-term  
370 measurements of airflow and turbulence in two street canyons in Manchester.  
371 *Atmospheric Environment* 38, 69-79.  
372

373 Oke, T.R., 1987. *Boundary layer climates*, second ed. Methuen, London, New York  
374 435pp.  
375

376 Rao, S.T., Sedefian L., Czapski U.H., 1979. Characteristics of turbulence and dispersion  
377 of pollutants near major highways. *Journal of Applied Meteorology* 18, 283-290.  
378

379 Rao, K.S., Gunter R.L., White J.R., Hosker R.P., 2002. Turbulence and dispersion  
380 modeling near highways. *Atmospheric Environment* 36, 4337-4346.  
381

382 Sedefian, L., Rao, S.T., Czapski, U., 1981. Effects of traffic-generated turbulence on  
383 near-field dispersion. *Atmospheric Environment* 15, 527-536.  
384

385 Stull, R., 1988. *An introduction to boundary layer meteorology*. Kluwer, Netherlands  
386 666pp.  
387

388 Sahlodin A.M., Sotudeh-Gharebagh R., Zhu Y., 2007. Modeling of dispersion near  
389 roadways based on the vehicle-induced turbulence concept. *Atmospheric Environment*  
390 41, 92-102.  
391

392 Tennekes, H., Lumley J.L., 1972. *A first course in turbulence*. The MIT Press,  
393 Cambridge, Massachusetts, London 300pp.  
394

395 Vachon, G., Louka, P., Rosant, J.M., Mestayer, P.G. and Sini, J.F., 2000. Measurements  
396 of traffic induced turbulence within a street canyon during the Nantes'99 experiment.



- 397 Proceedings of the Third International Conference on Urban Air Quality, Loutraki,  
398 Greece.  
399
- 400 Watkins S., Saunders J.W., Hoffmann P.H., 1995. Turbulence experienced by moving  
401 vehicles. Part I. Introduction and turbulence intensity. *Journal of Wind Engineering and*  
402 *Industrial Aerodynamics* 57, 1-17.  
403
- 404 Weiß, C., 2002. Untersuchungen zur autobahninduzierten Turbulenz. Universität  
405 Karlsruhe, Seminararbeit 39pp.  
406
- 407 Wang Y.J., Zhang K.M., 2009. Modeling near-road air quality using a computational  
408 fluid dynamics model, CFD-VIT-RIT. *Environmental Science & Technology*, 43,  
409 7778–7783.  
410
- 411 Wyngaard, J.C., 2010. *Turbulence in the Atmosphere*. Cambridge University Press.  
412 393pp.  
413
- 414 Xia J.Y., Leung D.Y.C., Hussaini M.Y., 2006. Numerical simulations of flow-field  
415 interactions between moving and stationary objects in idealized street canyon settings.  
416 *Journal of Fluids and Structures* 22, 315-326.  
417 **and vehicle speed.**